INTERNATIONAL JOURNAL OF GEOMATICS AND GEOSCIENCES
Volume 6, No 3, 2015

Research article ISSN 0976 – 4380

Drought Monitoring Using Remote Sensing Approaches: Western Desert , Egypt

Hala M. Ebaid
Associate professor , Survey Research Institute , National Water Research Center, Giza ,Egypt
hala_srif@yahoo.com

ABSTRACT

A new drought index was examined using Soil moisture(SM) and Land Surface temperature (LST) reflectance data, which deduced from Landsat images, called (LST/SM). This new index was examined beside other effective existing drought index named :Perpendicular Drought Index(PDI), which consider as useful indicator for monitoring drought condition . These indices were applied on the middle of western desert of Egypt (Kharga and Dakhla regions) as study areas. Red ,blue, and near- infrared wavelengths of landsat 8 (2014) and TM 5(2003) images were preprocessed : First geo-registed then converted to TOA Reflectance for SM , PDI indices determination Thermal infrared bands were processed using different algorithms to deduce LST data . 800 random points were well distributed on each resulted index raster image to analyze the drought condition. The results demonstrated that for Kharga region : the mean value for LST/SM index was slightly increased from 16.770 in 2003 to 16.807 in 2014, and for PDI index ,the mean value increase from 0.583 in 2003, to 0.6171 in 2014.For Dakhla region :mean value of LST/SM index increase from 17.589 in 2003 to 20.820 in 2014 , while for PDI index , the mean value increase from 0.5676 in 2003 to 0.6021 in 2014.. Analyzing the drought indices proved low correlation between LST/SM and PDI(r =.457). This may be due that both methods are different . The PDI method is based on utilizing two bands ie. Red and Infrared band while LST/SM is based on three bands which are Blue , Thermal , and infrared one .Again this low correlation coefficient may result from the different behavior of the two methods under the tested conditions. Finally, determining either PDI or LST/SM indices using satellite images provides simple and effective monitoring method in the remote estimation of drought phenomena.

Keywords: Drought index; LST/ SM ; PDI ; Landsat ; Western Desert; Egypt

1. Introduction

In the past, conventional drought monitoring approaches based on climatic and meteorological observations have been the primary tools for measuring the severity of droughts, for example, the Palmer Drought Severity Index (PDSI) (Palmer, 1965), the Rainfall Anomaly Index (RAI) (Van Rooy, 1965), the Crop Moisture Index (CMI) (Palmer, 1968), the Bhalme–Mooley Index (BMDI) (Bhalme and Mooley, 1980), the Surface Water Supply Index (SWI) (Shafer and Dezman, 1982), the Standardized Anomaly Index (SAI) (Katz and Glantz, 1986), the Standardized Precipitation Index (SPI) (McKee et al., 1993, 1995). But ground instruments used in conventional drought monitoring provide only localized estimates of most of the factors utilized to stand upon the drought condition such as soil moisture content, besides that their implementation is often expensive and time

consuming as well as labour-intensive and sometimes subject to instrument failure (G. Petropoulos, 2009).

Remote sensing has been proven to be a promising means for drought estimation over large areas in real time. A wide variety of drought monitoring models have been developed using various satellite data. They are typically based on satellite derived VIs, LST based methods and empirical methods using a certain combination of LST from thermal band data versus VIs from visible and near infrared data (Ghulam, A., 2006). Several studies have noted that the Normalized Difference Vegetation Index (NDVI) has the utility for observing droughts in time–series satellite data, (Di et al., 1994; Kogan, 1990; Liu and Ferreira, 1991). Vegetation Condition Index (VCI) (Kogan, 1995a) were also used to map both annual vegetation dynamics and drought patterns. As well as LST is a is one of the biophysical factors sensitive to surface water stress (Jackson et al., 1981).

Nevertheless, a simple, quantitative drought monitoring method that is robust over bare soil and varies with vegetation cover over different ecosystems, particularly in the term of soil moisture, is of great interest to those practicing precision agriculture. Taking the advantage of the reflective and absorptive features of the canopy and bare soils in the NIR and Red spectral domain, Ghulam et al. (2006) designed the Perpendicular Drought Index (PDI) using ETM+ imagery. As described by Ghulam et al. (2006), the PDI is very effective for bare soil applications, however, there are some limitations that challenge the performance of the PDI in areas whose surface cover types vary from bare soil to densely vegetated agricultural fields and are characterized by non-flat topography with different soil types. Despite the simplicity of the PDI method , yet it needs several steps to derivate the index such as the construction of spectral space and soil line, signatures points treatments, beside the application of several equations.

Therefore this paper is carried out to introduce another simple method to measure drought based on the combination of two important indicators of water stress that is land surface temperature (LST) and soil moisture(SM) data as compared to PDI method, using Landsat images applied on the Western Desert area for the years 2003 and 2014 to measure the changes in drought (if any)during this time.

2. Study area

Desertification is the consequence of a set of important processes, which are active in arid and semi-arid environment, where water is the main limiting factor of land use performance in ecosystems (Batterbury and Warren, 2001). In this study, two desert oases (Dakhla and Kharga regions) are located at the middle of western desert, Egypt, (Figure 1).The study areawhich comprises the two oasis expands from longitude of 28° to 32° in east, and latitude of 24° 50' to 27° in north. It covers a total area of 118 km^2. The Dakhla oasis is located 200 km northwest of Kharga. The desert climate is recognizable in all oases, the difference in day and night temperature degrees are vast especially in winter(Gad, 2007). Evapotranspiration rates are as high as 2.6 mm/day in January and up to 9.1 mm/day in June. Annual precipitation does not exceed 1 mm and rainy months are January and February (CLAC 2015).Wind speed ranges from 3 knots in December to 5.5 knots in June and the predominant wind direction is the north to north-west. There is a massive sand dune field; the Great Sand Sea, that extends to about 400 km north of the Dakhla depression. The majority of the population in Dakhla (about 70,000 persons) are working in farming and grazing. Water recourses are exclusively restricted to groundwater recharged from the Nubian

sandstone aquifer system. It is planned to restrain 200,000 persons in the depression relying on the groundwater reserves. Perennial vegetation is the date palm and olive however, vegetables and alfalfa are also cultivated. Soils of the Dakhla depression are classified as Calcisols (FAO/UNESCO 1977).

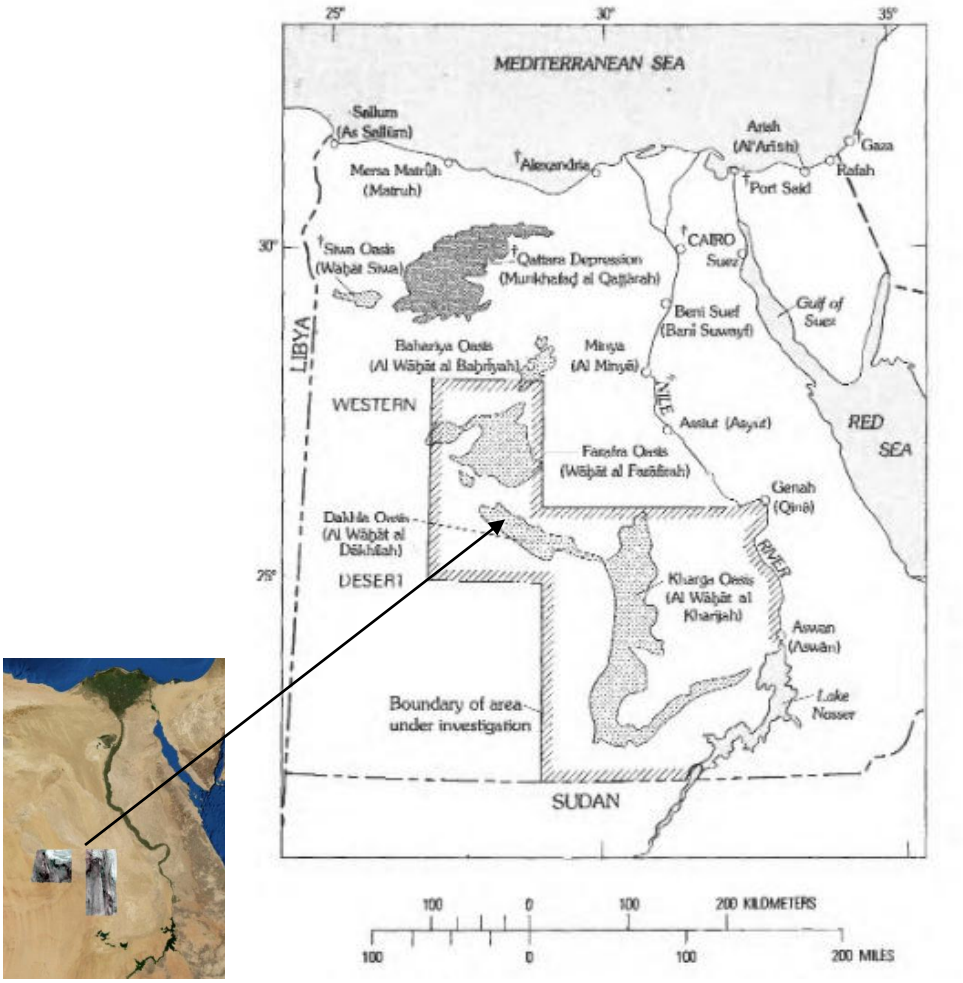

Figure 1: Study area

3. Data used

Four Landsat images with paths /rows: (177/42),(177/43),(176/42),(176/43) were used (the images were free and downloaded from: http://earthexplorer.usgs.gov)two images were used for each date (15/8/2003 and 15/8/2014) to monitor drought change during these two years . These two date were chosen for two reasons first : to be long time for change study , second for good images availability on internet . Particular bands were used in this study and demonstrated in table 1and 2.

Table 1: Landsat (TM5) Bands used for drought monitoring on 15/8/2003

Thematic Mapper (TM) and Thermal Infrared Images were acquired at 15/8/2003	Landsat 5	Wavelength (micrometers)	Resolution (meters)
	Band 1 (Blue band)	0.45-0.52	30
	Band 3 (Red band)	0.63-0.69	30
	Band 4 (NIR band)	0.76-0.90	30
	Band 6 (Thermal band)	10.40-12.50	30

Table 2: Landsat 8 Bands used for drought monitoring on 15/8/2014

Landsat 8 Operational Land Imager (OLI) and Thermal Infrared Sensor (TIRS) Images were acquired at 15/8/ 2014	Bands	Wavelength (micrometers)	Resolution (meters)
	Band 2 - Blue	0.45 - 0.51	30
	Band 4 - Red	0.64 - 0.67	30
	Band 5 - Near Infrared (NIR)	0.85 - 0.88	30
	Band 10 - Thermal Infrared (TIRS) 1	10.60 - 11.19	30
	Band 11 - Thermal Infrared (TIRS) 2	11.50 - 12.51	30

4. Methodology

Initial images processing included :
- A sub-images of the Kharga , Dakhla regions were cut after a layer stacking, mosaic processing , and geometric correction were carried out. All Digital Numbers (DNs) for proposed bands visible bands(Red ,Blue) and Near infra-red (NIR) were converted into a spectral radiance and then to top of the atmosphere (TOA) reflectance in two steps as follows :

a - Convert DN to radiance using gain and bias values using equation1 (http://landsathandbook.gsfc.nasa.gov/data_prod/prog):

$$L\lambda = \text{gain} * DN + \text{bias} \qquad (1)$$

Where: $L\lambda$ is the cell value as radiance , DN is the cell value in digital number, gain and bias are specific for a specific band (gain and bias parameters are found in header file with the landsat images) .

b - Convert Radiance to ToA Reflectance using equation 2 (http://landsathandbook.gsfc.nasa.gov/data_prod/prog):

$$\rho\lambda = \pi * L\lambda * d2 / ESUN\lambda * \cos \theta s \quad (2)$$

Where: ρλ is = unitless plantary reflectance; Lλ= spectral radiance (from earlier step); d is the Earth-Sun distance in astronmoical units; ESUNλ is the mean solar exoatmospheric irradiances ;θs is the solar zenith angle (all these parameter are found in header file).

- To estimate land surface temperature , the following procedures were carried out

i- Calculate At-Sensor Radiance
As objects will emit thermal electromagnetic energy as their temperature is above absolute zero (K), the signals received by the thermal sensors (TM/L8) can be converted to at-sensor radiance using equation 1.

where Lsensor(Lλ) is spectral radiance of thermal band in W/(m2 steradian mm) in radiance energy units; gain is the slope of the radiance/DN conversion function; DN is the digital number of a given pixel; and bias is the intercept of the radiance/DN conversion function (Landsat Project Science Office, 2002). The gain and bias values can be found in header files of TM 5 / L8 images.

ii- Calculate Brightness Temperature

Radiance values from the TM 5 / L8 thermal band were then transformed to radiant surface temperature, namely top-of-atmosphere brightness temperature, using thermal calibration constants according to Eq. (3) (http://landsathandbook.gsfc.nasa.gov/data_prod/prog):

$$T_{sensor} = \frac{K_2}{\ln\left(\frac{K_1}{L_{sensor}} + 1\right)} \quad (3)$$

where Tsensor is effective at-satellite temperature (brightness temperature) in K. K1 and K2 are prelaunch calibration constants and they are pre-settled. For Landsat 5 TM, K1=607.76 W/(m2 sr mm), and K2=1260.56K) (Landsat Project Science Office, 2002).
For TIRS bands data of Landsat 8 : k1=774.89 , k2= 1321.08 for b10 and k1=480.89 ,k2= 1201.14 for b11 . The temperature calculated by Eq. (3) is not the actual LST, but the top-of-atmosphere brightness temperature.

Deduced Land surface temperature from brightness temperature , and Emissivity *e* was carried out using equation 4(http://landsathandbook.gsfc.nasa.gov/data_prod/prog).

$$S_t = \frac{T_B}{1 + (\lambda \times T_B/\rho)\ln\varepsilon} \quad (4)$$

where: λ= wavelength of emitted radiance (for which the peak response and the average of the limiting wavelengths (Markham & Barker, 1985) will be used), $\rho = h*c/\sigma$ ($1.438*10^{-2}$ m K), σ = Boltzmann constant ($1.38*10^{-23}$ J/K), h = Planck's constant ($6.626*10^{-34}$ J s), and c = velocity of light ($2.998*10^{8}$ m/s) , ε is the emissivity for the two land cover radiance data .

4.1 Land surface temperature/ soil moisture index (LST/ SM) determination

There are three main contributors to drought: (1) land surface temperatures, (2) atmospheric circulation patterns, and (3) soil moisture content. Each of these physical parameters is linked to the others intricately; changing any one of them significantly will typically set up a chain of events that causes the other parameters to change. Sometimes, this chain of events becomes a vicious cycle in which the changing parameters, feeding off one another, are amplified to produce extreme climate conditions-such as drought(Trenberth and Guillemot 1996; Mo et al. 1997). TVX is consider as a suitable index for drought monitoring. It combines surface temperature and a normalized difference vegetation index and can be described as LST/NDVI,and this TVX, has been proven to be significantly correlated with soil moisture in most climatic and land cover conditions ,also it provides a better understanding of drought events in rapid and effective manner (McVicar and P. N. Bierwirth, 2001).Hence TVX index was the main reason to try and examine another index based also on two combinations considered as important indicator to asses drought phenomena ie. .land surface temperature and soil moisture which are deduced using Landsat bands. The resulted index is more suitable for soils prone to desertification. The increase in surface temperature causes a consequent decrease in soil moisture ,thus maximizing LST/SM value.

The soil moisture (in raster dataset format) was measured using the formula:

$$SM = NIR\ band / Blue\ band \qquad (5)$$

where SM stands for soil moisture ; NIR stand for near infrared band , and the blue band is a visible band.Near and short infrared bands have been described as being the best bands for water absorption . Their wavelengths were sensitive to water absorption and, as such, they were useful to indicate the moisture content. Blue band is known to provide water penetrating properties and to be able to differentiate between soil and vegetation. The deduction of LST is mentioned in the previous formulas 3 and 4.
The Land surface temperature/ soil moisture index (LST/ SM) was deduced using raster calculator (pixel by pixel for all raster dataset bands under Arc GIS environment model in one equation (6)).

$$LST/SM = (Surface\ temperature * Blue\ band) / IR\ band \qquad (6)$$

4.2 Perpendicular Drought Index (PDI)

Green vegetation exhibits strong absorption in Red spectral range and intensively reflects the NIR spectrum. The denser the vegetation, the smaller the reflectance is in the Red spectrum and the higher it becomes in the NIR bands. Reflectance in the Red range is below 3– 5%, while it reaches 40–60% in the NIR domain and, due to the absorption of the Red is saturated quickly, an increase of reflectance in the NIR region could only be the result of an further

increase in the density of vegetation (Gitelson, 2004). In the Red to NIR spectral domain, the reflectance of bare soil is high, but increases slowly. However, due to the strong absorption characteristics of water, bare soil reflectance decreases noticeably with increasing soil moisture, especially in the NIR region. Therefore, any mathematical operation in the form of ratio and subtraction that could strengthen the difference between the NIR and the Red could be used to describe the vegetation, surface drought status and would also be able to discriminate the soil information from the vegetated pixel. Additional narration of the NIR-Red spectral space characterized with spectral behavior of vegetation and soil moisture can be found in the work of Ghulam et al. (2006).

Considering the spectral characteristics of surface targets of: 1-Landsat ,Thematic Mapper:TM 5 (2003) , band 3(.63-.69 micrometers) , band 4(.76 -.9 micrometers) , and 2-the Landsat 8(2014) spectral features, the OLI band 4 (Red, .64– .67 micrometers) and band 5 (NIR, .85–.88 micrometers) , were selected to construct the NIR-Red spectral space for the two dates. In this study ,real scatter plots for landsat data was created (using Erdas Imagine S/W) for the atmospherically corrected NIR-Red reflectance spectrum, and it have been showed a typical triangular shape. Different land cover types manifested certain regular distributions in the NIR-Red spectral space. Not only the vegetation coverage can be described, but also the severity of the surface drought can be characterized quantitatively in the space (Figure2).

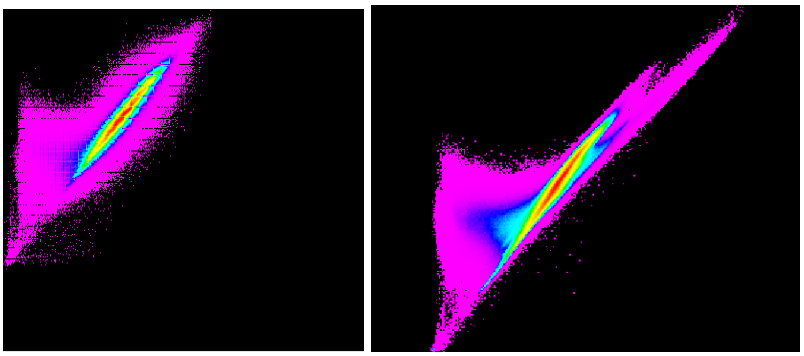

Figure 2: Construction of NIR–Red spectral space using:TM5 (2003) & Landsat 8 (2014)

It can be seen from figure 3 that the density distribution of vegetation in the space is similar with what Richardson and Wiegand (1977) reported. Here, the AD line represents the change of surface vegetation from the full cover (A) and the partial cover (E) to bare soil (D) while BC refers soil moisture status for wet area (B), semi-arid surface to extremely drought surface (C). As can be seen, BC shows the direction of drought severity. There are close but complex relationships between the surface spectrum and land cover types and surface drought conditions. This help to build a NIR–Red spectral reflectance space based drought monitoring index which may be rather simple and effective compared to the LST– NDVI and albedo-NDVI space based methods in which retrieval of albedo and LST is quite expensive and problematic. The soil line is made up of plots characterizing the spectral behavior of non-vegetated pixels and whose moisture varies obviously. It can be seen from the Figures3 that the drought severity gradually rises from B to C, and reaches its climax at C. Here BC represents the soil line of the research area, supposing that the mathematical expression of the soil line can be expressed by the following equation 7 (Ghulam, 2006).

$$R_{s,NIR} = M R_{s;red} + I . \quad (7)$$

Here, $R_{s,\ red}$, $R_{s,\ NIR}$ refer to the atmospherically corrected reflectance of NIR band and red band, respectively, while M refers to the slope of the soil line, I is the interception on the vertical axis. A line L, which disects the coordinate origin and is vertical to the soil line, can be delineated on Figure 3. Therefore, as to the normal function of a line, L can be mathematically formulated from the soil line expression(Ghulam, 2006).

$$R_{NIR} = -1/M\ R_{red}\ . \qquad (8)$$

For bare soil, the distance from any points in the NIR– Red reflectance space to the line L represents the drought severity of the non-vegetated surface. With the increasing amount of vegetation, the plots shift upward along the direction vertical to the soil line while they do the same along the direction parallel to the soil line and orthogonal to normal line L with the increasing of the soil moisture. For a vegetated surface, the distance from L to any points in the NIR–Red spectral space may indicate the drought severity of a mixed pixel. That is, the farther the distance, the stronger the drought, and the less the soil moisture or vice versa. Thereby, it is possible to formulate the drought severity using the mathematical expression of the distance from point to line. Taking a random point, a pixel E (R_{red}, R_{NIR}) in the NIR–Red reflectance space, the vertical distance from E (R_{red}, R_{NIR}) to line L (PDI) can be written as equation 9(Ghulam, 2006).

$$PDI = \frac{1}{\sqrt{M^2 + 1}}(R_{red} + MR_{NIR}). \qquad (9)$$

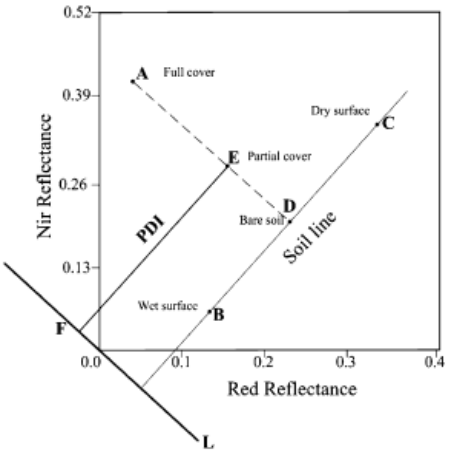

Figure 3: Sketch map of NIR-Red space and PDI.

With respect to a black body, the distance is the least amount which almost equals zero, and it is located just at the coordinate origin. In the case of other objects with some reflectance, the higher moisture content the target possesses, the nearer it is located to the coordinate origin. Generally speaking, objects placed near the line L are always bodies of water or are extremely wet regions and the drought value infinitely closes to 0, whereas in the most distant area from the line L in the space represents an extremely dry surface. In this case, drought value infinitely closes to 1. Some signatures points for wet soil and vegetation and bare soil were collected from original images and reflected on spectral feature space and it was described by different colors circles automatically (these circles were drown automatically when apply signatures for feature space analysis under Erdass Imagine software environment), supervised by ground truth (as shown in Figure 4) , and allocated to detect the

accurate soil line , vegetation line , and line L , from which the slope M were determined for the two dates .

.

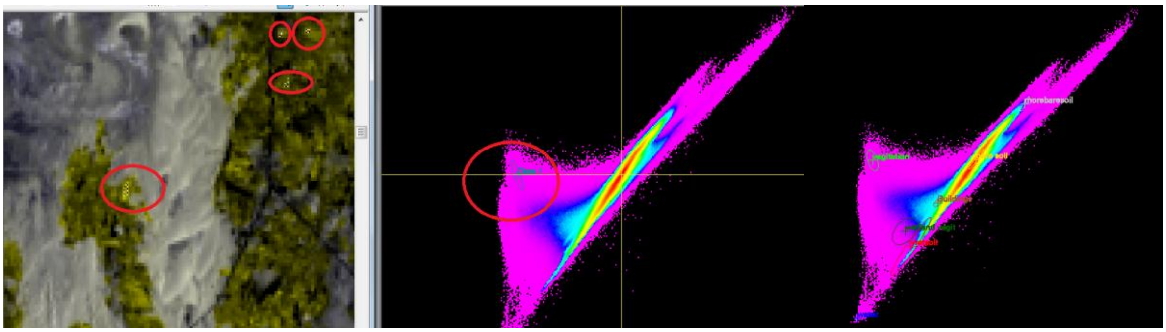

Figure 4: Signatures for Vegetation and bare soil and wet soil on Feature space scatter plot between Red and NIR wavelengths.

The slope M for real time drought index was deduce by applying simple geometry relation on the feature space, for date 2003: M= 1.2034 and, for date 2014 : M= 1.3451 (as shown in figure 5) . By Applying M value in equation 7,drought raster values can be determined at real time for the two study areas .

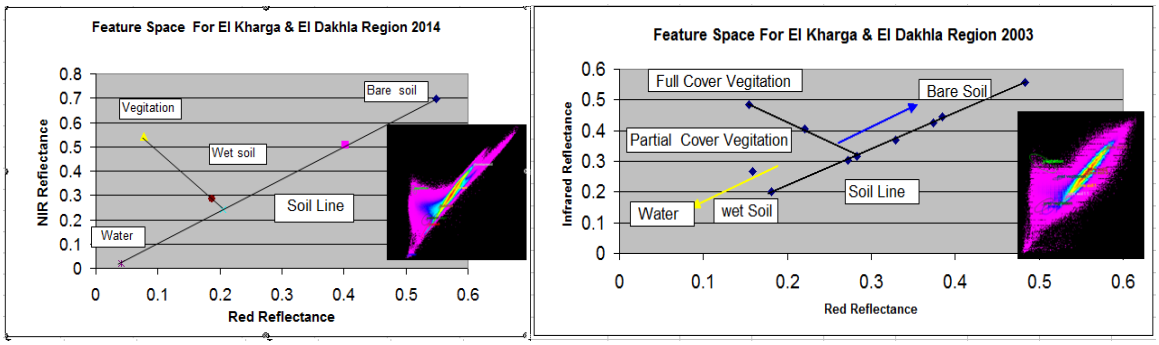

Figure 5: typical Slope of soil line (M) determine from spectral behavior of land cover

5. Results and Discussion

The above mention equations were carried out to determine the above mentions indices using GIS raster calculator tool. From the deduced drought maps using PDI or LST/SM indices, the drought severity levels information can be detected for each date. Drought values were slightly increased in 2014 using PDI and LST/SM techniques (Figure 6)

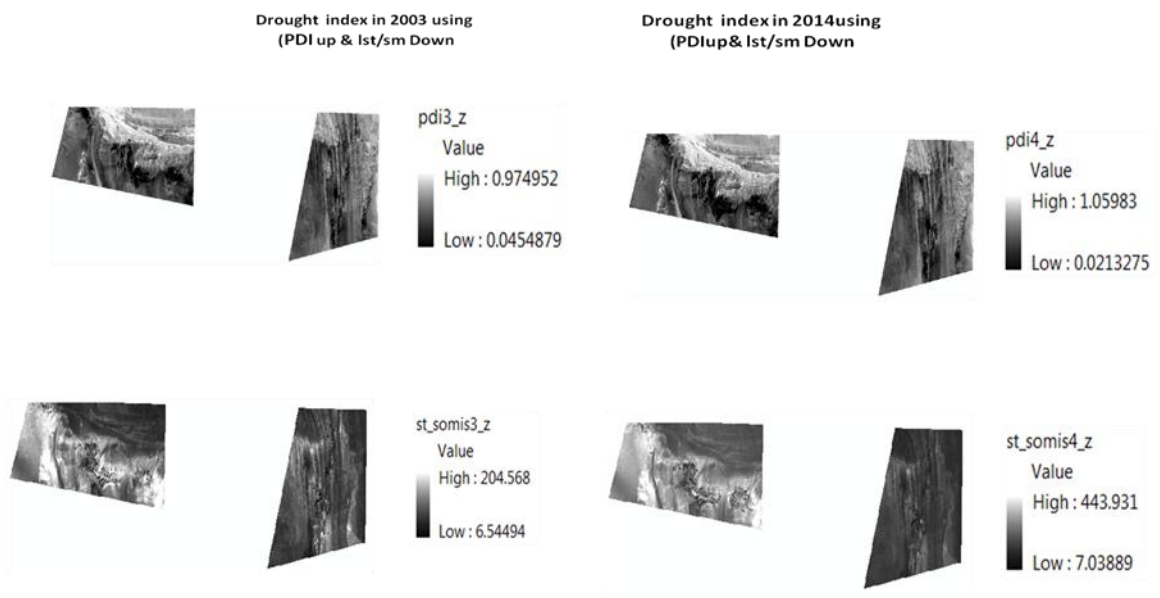

Figure 6: Output PDI index map (Up) & LST/SM index map (Down).

It is important to clear that LST/SM index detect the drought area from hydrological , and meteorological point of view, were it detect the drought areas based on shortage of soil moisture, and high values of land surface temperature if any , which will maximize the LST/ SM index values . The PDI is effective for bare soil applications, however, there are some limitations that challenge the performance of the PDI in areas whose surface cover types vary from bare soil to densely vegetated agricultural fields and are characterized by non-flat topography with different soil types. So combination of different existing indices like (LST/NDVI or VTCI or VCADI or the new index which was examined in this paper)may provide useful tools for better understanding of the spatio-temporal patterns of drought. For desert environment , and land cover nature of this specific areas, which characterized by its bare soil, and little cultivated areas , it will be better to distribute random points to extract corresponding drought values, hence analyzing drought condition over the study areas . By using ArcGIS ,1600 random points were well distributed over drought raster images for Dakhla and Kharga study areas, and corresponding drought pixels value were determined(by extract the cell values of a raster based on these random points and records the values in attribute table of an shape file using tool "extract values to points" under ArcGIS 10.2 environment) . Statistical parameters were calculated and demonstrated in tables 3 and 4. .The mean value for LST/SM index slightly increased from 16.770 in 2003 to 16.807 in 2014, and for PDI index :the mean value increase from 0.583, to 0.6171 for Kharga region .For Dakhla region :mean value of LST/SM index increase from 17.589 to 20.820 , while mean value of PDI index increase from 0.5676 in 2003 to 0.6021 in 2014. Standard deviation (SD) for LST/SM index were increased from 2.5933 in 2003 to 2.9775 in 2014 for Kharga region , and SD increase from 2.9996 in 2003 to 3.0756 in 2014 for Dakhla region .The correlation coefficient between the two indices LST/SM and PDI proved to be low (r =.457).This may be due that both methods are different . The PDI method is based on utilizing two bands ie. Red and Infrared band while LST/SM is based on three bands which are Blue , Thermal , and infrared one.Figure 7 shows increasing in drought levels in Dakhla *region* based on PDI index values, were the circle shows little bit change in colour from orange to yellow or the little bit change of drought index PDI values as demonstrated by the following map .

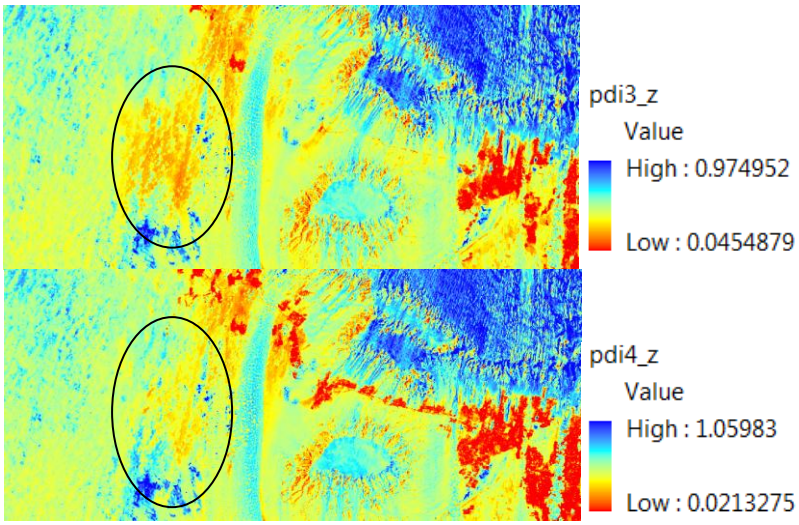

Figure 7: The drought increase in particular areas from 2003 to 2014 (Based on PDI index map)

Drought maps for Dakhla region were deduced also from LST/ SM index raster data, and increasing in drought levels were noticed in the upper right side , lower left side, and other areas of Dakhla region as shown in Figure 8 .

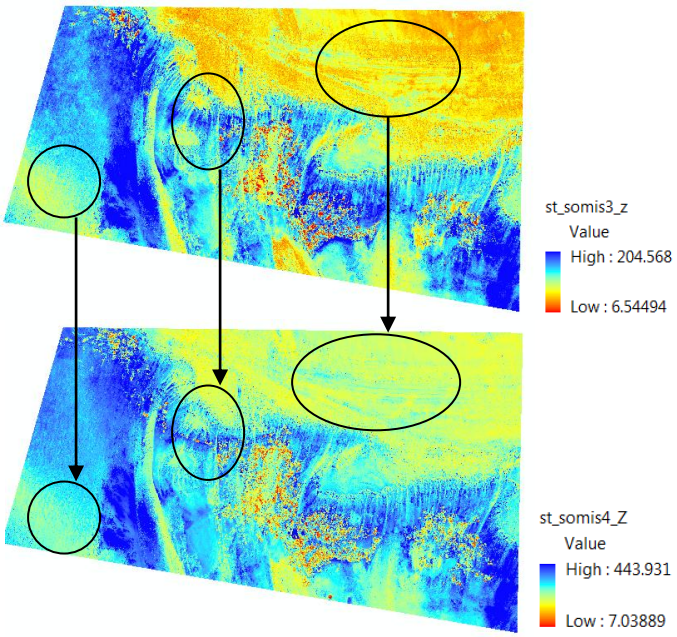

Figure 8 : The drought increased slightly in particular areas from date 2003 to 2014 (based on LST/ SM index map)

For evaluation for this work , ground truth data are needed , but unfortunately this data is not available , and based on Gad (2007) the resulted drought map is based on real field data . The trend of drought distribution for the present study is almost similar to that of Gad (2007) where the color blue and cyan describe the higher drought index as the dark brown area of Gad (2007) for both areas ,Dakhla and Kharga (Figure 9).

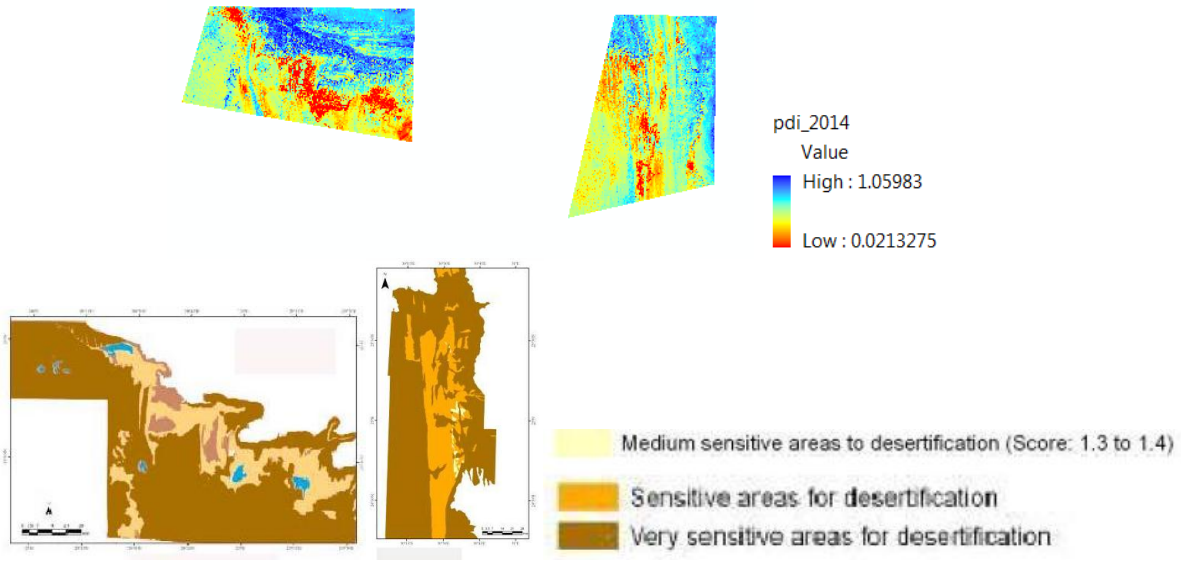

Figure 9: Resulted Drought map by author (Up) & Resulted Drought map by Gad 2007 (Down)

Table 3: Statistic parameters for Drought Index values (Dakhla region)

Study area Dakhla region	**Statistical parameters**	**PDI**	**Land Surface Temperature/Soil moisture (LST / SM)**
	Max value 2003	0.80434	31.045216
	Max value 2014	0.89154	31.669411
	Min value 2003	0.17989	11.568535
	Min value 2014	0.22234	10.825859
	Mean 2003	0.5676	17.589123
	Mean 2014	0.60193	20.820315
	S. D. 2003	0.07850	2.999641
	S.D. 2014	0.08876	3.075577

Table 4: Statistic parameters for Drought Index values (Kharga region)

Study area	**Statistical parameters**	**PDI**	**Land Surface Temperature/Soil moisture (LST / SM)**
Kharga region	Max value 2003	0.7794	27.86343
	Max value	1.03197	29.01181

	2014		
	Min value 2003	0.337	-31.79624
	Min value 2014	0.2561	-8.86626
	Mean 2003	0.5834	16.769869
	Mean 2014	0.6171	16.806857
	S. D. 2003	0.0563	2.593319
	S.D. 2014	0.07263	2.977452

5.1 Conclusion

The application of PDI index in Kharga and Dakhla in the western desert of Egypt for the years 2003 and 2014 to asses the change in drought condition showed slight increase in drought index , with mean values of 0.58 in 2003 and .61 in 2014. Another index ie. LST/SM was also tested on the same area and resulted in slight increase, averaging from 17.36 in 2003 to 18.37 in 2014. Also a correlation coefficient between the two indices LST/SM and PDI proved to be low (r =.457).This may be due that both methods are different . The PDI method is based on utilizing two bands ie. Red and Infrared band while LST/SM is based on three bands which are Blue , Thermal , and infrared one .Again this low correlation coefficient may result from the different behavior of the two methods under the tested conditions . It can be concluded that LST/ SM method is more simple than the PDI one, as it does not need several steps to derivate the index such as the construction of spectral space and soil line, and the taken several signatures from the images , besides the application of several equations which are used with the PDI method .However the new index (LST/SM) need to be further studied and future work should focus to handle and improve its performance.

6. References

1. Batterbury, S.P.J. & A.Warren. (2001). Desertification. in N. Smelser & P. Baltes (eds.) International Encyclopedia of the Social and Behavioral Sciences. Elsevier PressPp. 3526-3529.

2. Bhalme, H.N., Mooley, D.A., 1980. Large-scale droughts/floods and monsoon circulation. Monthly Weather Review 108 (8), 1197–1211.

3. CLAC Central Laboratory for Agricultural Climate. 2015. Summaries of climatic normals Cairo: The Ministry of Agriculture. Available from:www.calc.edu.org

4. Di, L., Rundquist, D.C., Han, L., 1994. Modeling relationships between NDBI and precipitation during growth cycle. International Journal of Remote Sensing 15 (10), 2121–2136.

5. FAO-UNESCO (1977) FAO-UNESCO Soil Map of the World, Vol. VI. Africa. UNESCO, Paris, 299.

6. Gad, A. 2007. Combined GIS and Remote Sensing techniques in Mapping Desertification Sensitivity in the North of the Western Desert, Egypt, the Second National GIS Symposium in Saudi Arabia, Al-Khobar, Kingdom of Saudi Arabia, April 23-25, 2007 / Rabi II 6-8, 1428.

7. Gitelson, A.A., 2004.Wide dynamic range vegetation index for remote quantification of biophysical characteristics of vegetation. Journal of Plant Physiology 161 (2), 165–173.

8. Ghulam, A., Qin, Q., Zhan, Z., 2006. Designing of the perpendicular drought index. Environmental Geology. doi:10.1007/s00254-006- 0544-2.

9. Ghulam, A., 2006. Remote monitoring of farmland drought based n-dimensional spectral feature space. PhD dissertation (in Chinese), Peking University, Beijing.

10. http://landsathandbook.gsfc.nasa.gov/data_prod/prog.

11. Jackson, R.D., Idso, S.B., Reginato, R.J., Pinter Jr., P.J., 1981. Canopy temperature as a crop water stress indicator. Water Resources Research 17 (4), 1133–1138.

12. Katz, R.W., Glantz, M.H., 1986. Anatomy of a rainfall index. Monthly Weather Review 114 (4), 764–771.

13. Kogan, F.N., 1990. Remote sensing of weather impacts on vegetation in non-homogeneous areas. International Journal of Remote Sensing 11 (8), 1405–1419.

14. Kogan, F.N., 1995a. Droughts of the late 1980s in the United States as derived from NOAA polar-orbiting satellite data. Bulletin of the American Meteorological Society 76 (5), 655–668.

15. Landsat Project Science Office, 2002. Landsat 7 Science Data User's Handbook. Goddard Space Flight Center, GreenbeltMD.

16. Liu, W., Ferreira, A., 1991. Monitoring crop production regions in the Sao Paulo State of Brazil using normalized difference vegetation index. Proc. 24th. International Symposium on Remote Sensing of Environment, Rio de Janeiro, Brazil, vol. 2, pp. 447 455. 27–31 May.

17. McKee, T.B., Doesken, N.J., Kleist, J., 1993. The relationship of drought frequency and duration to time scales. Proc. Eighth Conference on Applied Climatology, American Meteorological Society, Anaheim, CA, pp. 179–184. 17–22 January.

18. Mckee, T.B., Doeskin, N.J., Kleist, J., 1995. Drought monitoring with multiple time scales. Proc. Ninth Conference on Applied Climatology, American Meteorological Society, Boston, MA, pp. 233–236. 15–20 January.

19. McVicar T. R. and Bierwirth, P. N., "Rapidly assessing the 1997 drought in Papua New Guinea using composite AVHRR imagery," International Journal of Remote Sensing, vol. 22, no. 11, pp. 2109–2128, 2001.

20. Mo, K., J. Nogués-Paegle and R.W. Higgins, 1997: Atmospheric processes associated with summer floods and droughts in the central United States. J. Climate , 10 , 3028 - 3046.

21. Palmer, W.C., 1965. Meteorological drought. Research Paper, vol. 45. U.S. Department of Commerce Weather Bureau, Washington, DC.

22. Palmer, W.C., 1968. Keeping track of crop moisture conditions, nationwide: the crop moisture index.Weatherwise 21 (4), 156–161.

23. Petropoulos, G., Carlson, T.N., Wooster, M.J. and S. Islam, 2009. A review of T s /VI remote sensing based methods for the retrieval of land surface energy fluxes and soil surface moisture Progress in Physical Geography 33(2) (2009) pp. 224–250.

24. Richardson, A. J., and Wiegand, C. L. (1977), Distinguishing vegetation from soil back- ground information, Photogramm. Eng. Remote sensing. 43:1541--1552.

25. Shafer, B.A., Dezman, L.E., 1982. Development of a surface water supply index (SWSI) to assess the severity of drought conditions in snowpack runoff areas. Proc. 50th AnnualWestern Snow Conference, Colorado State University, Fort Collins, CO, USA, pp. 164–175. 19–23 April.

26. Trenberth, K. E., 1998: Atmospheric moisture residence times and cycling: Implications for rainfall rates with climate change. , 39, 667–694

27. Van Rooy, M.P., 1965. A rainfall anomaly index independent of time and space. Notes 14, 43–48.